

## Spin-Dependent Superelastic Scattering from Pure Angular Momentum States of Na( $3P$ )

J. J. McClelland, M. H. Kelley, and R. J. Celotta

*Radiation Physics Division, National Bureau of Standards, Gaithersburg, Maryland 20899*

(Received 30 January 1986)

Spin asymmetries are presented for superelastic scattering of spin-polarized electrons from spin-polarized  $M_L = +1$  and  $M_L = -1$  states of the Na  $3P_{3/2}$  atom. The incident-energy dependence at a scattering angle of  $30^\circ$  is shown for energies of 1.26 to 11.76 eV. In addition, angular dependences over the range  $5^\circ$  to  $40^\circ$  are given at 2.0 and 9.26 eV. Large differences are seen between the spin asymmetries for the two  $M_L$  sublevels of the excited state, with the  $M_L = -1$  asymmetry reaching a value of 100% at 2 eV and  $35^\circ$  scattering angle, corresponding to pure singlet scattering.

PACS numbers: 34.80.Nz, 34.80.Qb

The investigation of low-energy electron scattering from atomic targets has suffered in the past from an experimental inability to resolve all the independent predictions of theoretical models. Typically, a comparison between theory and cross-section measurements involves an average over at least two and often many more independent channels. Such averaging can often obscure discrepancies between theory and experiment, and so it is desirable to resolve experimentally as many of the separate channels as possible. Only then can a complete test of theory be achieved.<sup>1</sup>

In spite of the direct value of such measurements for the understanding or evaluating of theoretical models, only limited experimental separation of individual scattering channels has been accomplished to date. In the past this work has for the most part concentrated on either of two areas. Separation of spin channels by use of spin-polarized electrons and targets has led to investigations of the roles played by such spin-dependent effects as spin-orbit coupling and exchange.<sup>2,3</sup> Separation of target angular momentum channels for inelastic scattering has been accomplished by observation of either superelastic scattering or coincidences between scattered electrons and emitted photons.<sup>4</sup> Recently, the first spin-polarized electron-photon coincidence experiment was performed<sup>5</sup> on a spin-0 target (Hg). The present work represents the first superelastic scattering experiment where the spins of both the incoming electron and target atom are polarized. We report a study of a spin- $\frac{1}{2}$  target in which we measure as a function of incident energy and scattering angle the separation of the scattering into singlet and triplet channels for each of the angular momentum states in the excited state of the target.

The particular inelastic scattering process studied is the one in which a scattered electron causes a transition in a sodium atom between the  $3S$  ground state and the  $3P$  first excited state. With the conventional assumption that the nuclear spin of the target atom plays no significant dynamic role during the interaction,<sup>6</sup> and with the further assumption that there is negligible continuum spin-orbit interaction for the scattered elec-

tron, one finds that four independent complex scattering amplitudes are required to characterize this scattering process completely. The squared magnitudes of these scattering amplitudes represent the transition probabilities for excitation of specific  $M_L$  states of the excited  $3P$  level, with the spins of the incident electron and atom forming a singlet or a triplet state.

In order to determine as much as possible about these four scattering amplitudes, the experiment must be able to resolve spins (to separate singlet and triplet contributions), and also to probe the  $M_L$  states of the excited atom. The former can be achieved by scattering of spin-polarized electrons from spin-polarized atoms. The latter can be effected either by use of photon-electron coincidence techniques,<sup>7</sup> or by measurement of the time-inverse, superelastic scattering process. When experimentally practical, superelastic scattering has an advantage over coincidence techniques because the counting rates are typically several orders of magnitude higher. Furthermore, the state selection inherent in the excitation process ensures that the transitions studied are transitions between well-characterized pure quantum states.

In superelastic scattering, a well-defined  $M_L$  population is created prior to the collision by excitation of the atoms with laser light of definite polarization.<sup>8</sup> Measurement of the cross section for deexcitation of this definite excited state is exactly equivalent to measuring the probability of its excitation. In sodium, when circularly polarized light tuned to the  $3S_{1/2}(F=2) \rightarrow 3P_{3/2}(F=3)$  transition is used, optical pumping results in an excited state which is purely  $M_F = +3$  ( $\sigma_+$  light) or  $M_F = -3$  ( $\sigma_-$  light). Such a state is a pure angular momentum state of the atom, consisting of maximal projections along the direction of laser propagation of the nuclear spin ( $M_I = \pm \frac{3}{2}$ ), the orbital angular momentum ( $M_L = \pm 1$ ), and the spin of the atomic electron ( $M_S = \pm \frac{1}{2}$ ). The fact that the nuclear spin is polarized is immaterial in the context of low-energy electron scattering, but the fact that the  $M_L$  states are pure means that their scattering contributions can be measured independently. If the ex-

Work of the U. S. Government

Not subject to U. S. copyright

periment is performed with the laser light incident perpendicular to the scattering plane, determination of the  $M_L = \pm 1$  scattering amplitudes constitutes a complete measurement, because the amplitude for  $M_L = 0$  is identically zero. (This state has its angular momentum vector lying in the scattering plane and hence cannot be excited or deexcited by the scattered electron, which has angular momentum only perpendicular to the scattering plane).

The addition of spin-polarized incident electrons to the superelastic scattering experiment allows one not only to measure separately the  $M_L = \pm 1$  contributions, but also to take advantage of the pure  $M_S$  state of the target electron. Measurements can be made with incident electrons polarized either parallel to the target electron spin, in which case the scattering is purely triplet in nature, or antiparallel, in which case the scattering has equal contributions from singlet and triplet states. Thus the  $M_L = +1$  and  $-1$  scattering intensities can be broken down into their singlet and triplet components.

The present experimental results are given in terms of two spin asymmetries, one for each  $M_L$  state. They are derived from scattering intensities via the formula

$$A = \frac{1}{P_e} \frac{I_{\uparrow\downarrow} - I_{\uparrow\uparrow}}{I_{\uparrow\downarrow} + I_{\uparrow\uparrow}}, \quad (1)$$

where  $P_e$  is the polarization of the incident electrons, and  $I$  is the scattering intensity for parallel ( $\uparrow\uparrow$ ) or antiparallel ( $\uparrow\downarrow$ ) electron spins. The asymmetry (1) has the advantage that it retains all the information unique to a spin-dependent experiment, while normalizing out any variations in the spin-averaged cross section. This normalization makes the asymmetry relatively insensitive to experimental artifacts that can arise from variations in electron beam intensity, atom beam density, beam overlap integral, or detection efficiency. Hence such asymmetries are very suitable experimental variables for rigorous comparison with theory. In terms of the two singlet and two triplet scattering amplitudes  $S_{+1}, S_{-1}$  and  $T_{+1}, T_{-1}$  for excitation of the  $M_L = +1$  and  $-1$  states, one can show that the two measured asymmetries are given by

$$A_i = \frac{|S_i|^2 - |T_i|^2}{|S_i|^2 + 3|T_i|^2}, \quad (2)$$

where  $i$  is  $+1$  or  $-1$ , corresponding to the  $M_L$  value. It is seen that this asymmetry can range from  $+1$ , when the scattering is purely singlet, to  $-\frac{1}{3}$ , when triplet dominates completely. We note in passing that  $A_{\pm 1}$  can also be expressed in terms of the perhaps more familiar direct and exchange amplitudes<sup>2</sup>  $f_{\pm 1}$  and  $g_{\pm 1}$  by the simple substitutions  $S = f + g$  and  $T = f - g$ .

The scattering geometry of the present experiment

is shown in Fig. 1. The experimental apparatus is essentially the same as was used in previous work, in which spin asymmetry was observed in superelastic scattering with linearly polarized excitation of the atoms.<sup>9</sup> A complete description of the apparatus will be published in the near future.

Polarized electrons are produced in a GaAs negative-electron-affinity photoemission source<sup>10</sup> with a polarization of about 25%. These electrons are formed into a nominally 2-mm-diam horizontal beam with energy 1–12 eV and energy spread of about 0.1 eV. The energy of the electron beam was calibrated by our configuring the detection system to measure positive ions and measuring the onset of electron impact ionization of sodium at 5.14 eV. The electron beam intersects a horizontal sodium beam of density about  $10^{10}$  atoms/cm<sup>3</sup> produced in an effusive recirculating oven. The intersection of the two beams defines the center of a horizontal scattering plane, in which rotates a channel electron multiplier equipped with a retarding-field energy analyzer. The electron polarization is transverse, oriented either “up” or “down” relative to the scattering plane. The voltage on the retarding element of this analyzer is set approximately 1 V above the incident electron energy, a level which is sufficient to reject all elastically and inelastically scattered electrons, but which allows the 2.1 eV more energetic superelastic electrons to reach the detector. A frequency-stabilized dye laser produces laser light which is circularly polarized either clockwise or counterclockwise and then directed into the scattering center from above. The frequency of the laser is locked to the  $3S_{1/2}(F=2) \rightarrow 3P_{3/2}(F=3)$  transition with a Doppler-shift-sensitive feedback mechanism.<sup>11</sup> Typical computer-controlled measurement protocol consists of modulating the spin of the electron beam at a frequency of 100 Hz and counting the scattered electrons separately for each incident electron spin with two gated scalars. At intervals of 1–10 sec, the laser

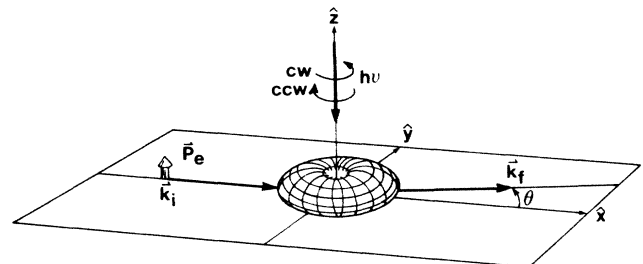


FIG. 1. Schematic of the scattering geometry, showing a representation of the charge density of the prepared  $3P$  state. The initial atomic state is prepared with circularly polarized light incident perpendicular to the scattering plane. Electrons with spin polarization  $P_e$  perpendicular to the scattering plane are incident with momentum  $k_i$  and scatter into an angle  $\theta$  with momentum  $k_f$ .

polarization is reversed, or the laser is blocked with a shutter to measure a background counting rate. Clockwise and counterclockwise counting rates for spin-up and spin-down incident electrons, as well as background counting rates, are averaged separately over typically 1 h of data acquisition time. The background is subtracted and two asymmetries are calculated from Eq. (1), one for each polarization of the incident light. The data presented in Figs. 2 and 3 represent averages over three such 1-h measurements for each incident electron energy and scattering angle.

The counting-statistics error estimates for the background and signal counting rates are propagated through the expression for the asymmetry to yield the 1-standard-deviation error bars shown in the figures. These error estimates are consistent with the reproducibility of the measurement as determined by the three separate 1-h measurements for each point. Not included in the error bars of the figures is a possible systematic error of  $\pm 6\%$  in the electron-spin polarimeter calibration.<sup>12</sup> Because this error is a normalization error which affects each point equivalently, it does not affect the relative precision of the data points.

Figures 2 and 3 show the behavior of the two spin asymmetries  $A_+$  and  $A_-$  as functions of incident-electron energy at a fixed scattering angle of  $30^\circ$  (Fig. 2) and as functions of scattering angle for incident energies of 2 eV [Fig. 3(a)] and 9.26 eV [Fig. 3(b)]. The difference between  $A_+$  and  $A_-$  is quite striking in all cases, especially considering the fact that the  $M_L = +1$  and  $-1$  states have identical charge distributions (represented schematically in Fig. 1). The difference between the two can be rationalized, however, by recognizing that the unpolarized cross sections are also quite different for  $M_L = +1$  and  $-1$ .<sup>13,14</sup> In fact, the

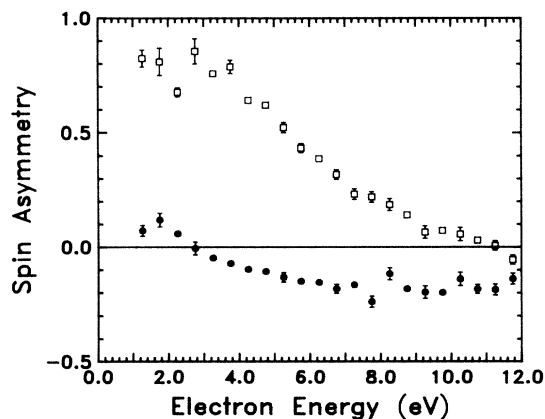


FIG. 2. Spin asymmetries  $A_+$  (circles) and  $A_-$  (squares) vs incident electron energy for superelastic scattering from the  $M_L = +1$  and  $M_L = -1$  states of Na ( $3P_{3/2}$ ). The scattering angle  $\theta$  is  $30^\circ$ . Error bars are 1 standard deviation derived from counting statistics and are shown only when they exceed the symbol size.

cross section for  $M_L = +1$  has been measured to be as much as 13 times that for  $M_L = -1$ .<sup>15</sup>

A classical analogy may help to understand such differences in cross section through consideration of the angular momentum transferred during the collision. While scattering to the "left," the scattered electron must gain angular momentum if it deexcites the  $M_L = +1$  state, while it must lose angular momentum on deexciting the  $M_L = -1$  state. Because the scattered electron gains energy from the superelastic collision, it is relatively easy to gain angular momentum, but losing angular momentum can only be accomplished through a large change in impact parameter. Thus, in this classical analogy, electrons deexciting the  $M_L = +1$  and  $M_L = -1$  atomic states must follow different classical trajectories through the atomic charge cloud. This difference makes plausible the difference in cross sections and also, because of the sensitivity of the exchange interaction to the region of the charge cloud probed, accounts for the widely different spin asymmetries.

From symmetry considerations, assuming parity conservation, one expects that scattering to negative angles should be the same as scattering to positive angles if both the incident-electron spin and the helicity of the exciting laser light are reversed. As a check for

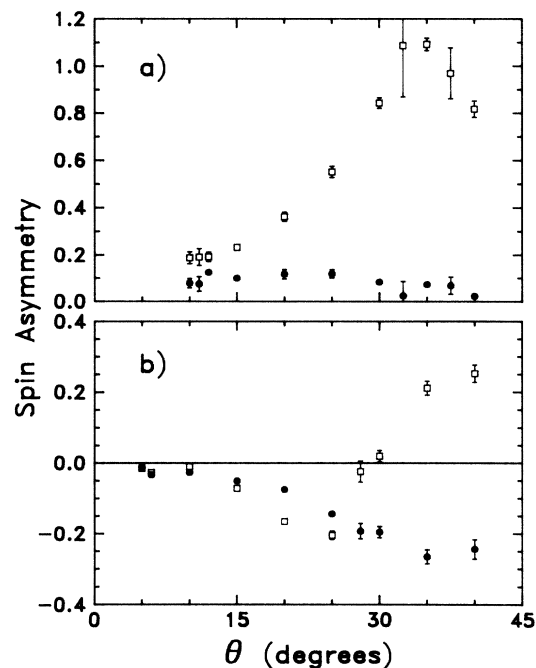


FIG. 3. Spin asymmetries  $A_+$  (circles) and  $A_-$  (squares) vs scattering angle for superelastic scattering from the  $M_L = +1$  and  $M_L = -1$  states of Na ( $3P_{3/2}$ ). (a) 2.0 eV incident-electron energy; (b) 9.26 eV incident-electron energy. Error bars are 1 standard deviation derived from counting statistics and are shown only when they exceed the symbol size.

instrumental asymmetries, we have investigated this and found it to be true. The data shown in Fig. 3 represent averages over positive and negative scattering angles.

The behavior of the spin asymmetries as a function of incident energy and scattering angle has several surprising features. Figure 2 shows a general trend in  $A_-$  from almost completely singlet scattering at low energies to nearly equal amounts of singlet and triplet at higher energies.  $A_+$  also starts out with somewhat more singlet, but rapidly becomes triplet dominated (recall that a value of  $-\frac{1}{3}$  indicates pure triplet scattering), and seems to be relatively constant in energy. The angular dependences displayed in Fig. 3 show that  $A_+$  has relatively smooth behavior as a function of scattering angle, while  $A_-$  has some very dramatic features. At 2-eV incident energy [Fig. 3(a)],  $A_-$  reaches its maximum possible value of 1.0 near  $35^\circ$ . This corresponds to a zero in the triplet scattering cross section. (It should be remarked that the measured maximum value of  $1.09 \pm 0.03$  is consistent with a value of 1.0 when the scale-factor uncertainty of 6% is taken into account.) At 9.26 eV [Fig. 3(b)], on the other hand,  $A_-$  shows a rapid sign change near  $30^\circ$ , going from almost all triplet to singlet domination within  $5^\circ$  of scattering angle.

The extreme value of  $A_-$  at 2 eV and  $35^\circ$  scattering angle, and its rapid variation at 9.26 eV and  $30^\circ$  scattering angle, as well as the overall shape of all the curves, provide new insight into the details of sodium  $3S \rightarrow 3P$  inelastic scattering and should provide challenging tests for theory. As yet, we know of no theoretical predictions for the asymmetries represented here, although it should be possible to compare both existing and new calculations with these data by use of Eq. (2). It is hoped that in the near future, rigorous comparisons between these data and theoretical predictions will facilitate the emergence of a new

understanding of the details of inelastic electron-atom scattering.

This work is supported in part by U. S. Department of Energy, Office of Basic Energy Sciences, Division of Chemical Science.

<sup>1</sup>B. Bederson, *Comments At. Mol. Phys.* **1**, 65 (1969).

<sup>2</sup>J. Kessler, *Polarized Electrons*, (Springer-Verlag, New York, 1986), 2nd ed.

<sup>3</sup>G. F. Hanne, *Phys. Rep.* **95**, 95 (1981).

<sup>4</sup>N. Andersen, J. W. Gallagher, and I. V. Hertel, in *Abstracts of Contributed Papers, Fourteenth International Conference on the Physics of Electronic and Atomic Collisions*, Palo Alto, 1985, edited by M. G. Coggiola, D. L. Huestis, and R. P. Saxon (North-Holland, Amsterdam, to be published), and references therein.

<sup>5</sup>A. Wolcke, J. Goeke, G. F. Hanne, J. Kessler, W. Vollmer, K. Bartschat, and K. Blum, *Phys. Rev. Lett.* **52**, 1108 (1984).

<sup>6</sup>I. C. Percival and M. J. Seaton, *Philos. Trans. Roy. Soc. London, Ser. A* **251**, 113 (1958).

<sup>7</sup>See, for example, *Coherence and Correlation in Atomic Collisions*, edited by H. Kleinpoppen and J. F. Williams (Plenum, New York, 1980).

<sup>8</sup>I. V. Hertel and W. Stoll, *Adv. At. Mol. Phys.* **13**, 113 (1978).

<sup>9</sup>J. J. McClelland, M. H. Kelley, and R. J. Celotta, *Phys. Rev. Lett.* **55**, 688 (1985).

<sup>10</sup>D. T. Pierce, R. J. Celotta, G.-C. Wang, W. N. Unertl, A. Galejs, C. E. Kuyatt, and S. R. Mielczarek, *Rev. Sci. Instrum.* **51**, 478 (1980).

<sup>11</sup>J. J. McClelland and M. H. Kelley, *Phys. Rev. A* **31**, 3704 (1985).

<sup>12</sup>L. G. Gray, M. W. Hart, F. B. Dunning, and G. K. Walters, *Rev. Sci. Instrum.* **55**, 88 (1984).

<sup>13</sup>M. Kohmoto and U. Fano, *J. Phys. B* **14**, L447 (1980).

<sup>14</sup>H. W. Hermann, I. V. Hertel, and M. H. Kelley, *J. Phys. B* **13**, 3465 (1980).

<sup>15</sup>J. J. McClelland, M. H. Kelley, and R. J. Celotta, to be published.